Biophysical Chemistry 228 (2017) 55–61

Contents lists available at ScienceDirect

Biophysical Chemistry

journal homepage: www.elsevier.com/locate/biophyschem

Binding kinetics of mutant p53R175H with wild type p53 and p63: A Surface Plasmon Resonance and Atomic Force Spectroscopy study

Ilaria Moscetti, Anna Rita Bizzarri, Salvatore Cannistraro*

Biophysics & Nanoscience Centre, DEB, Università della Tuscia, Viterbo, Italy

HIGHLIGHTS

- SPR and AFS monitored the high affinity complex of p53R175H and p53wt or p63.
- Mutant p53R175H interacts with all p53 family (p53, p63 and p73) with high affinity.
- Measured kinetics are insightful to drug design inhibiting these complexes.

GRAPHICAL ABSTRACT

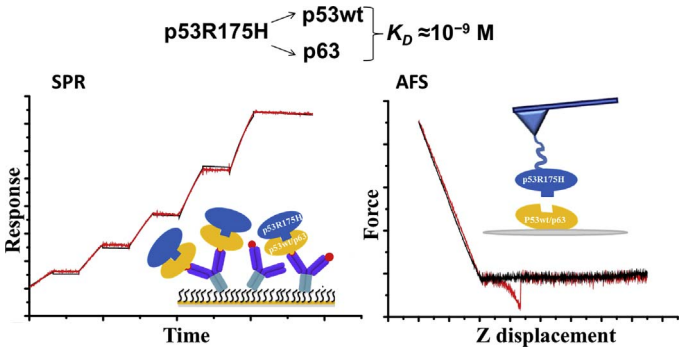

ARTICLE INFO

Keywords:
p53
p63
Surface Plasmon Resonance
AFS
p53R175H
Protein-protein interaction

ABSTRACT

The oncogenic mutant p53R175H, one of the most frequently occurring in human cancers and usually associated with poor prognosis and chemo resistance, can exert a dominant negative effect over p53 family members, namely wild type p53, p63 and p73, inhibiting their oncosuppressive function. Novel anticancer strategies based on drugs able to prevent the formation of complexes between p53R175H and the p53 family members call for a deeper knowledge on the molecular mechanisms of their interaction. To this aim, p53R175H/p63 and p53R175H/p53 complexes were investigated *in vitro* by using Surface Plasmon Resonance and Atomic Force Spectroscopy, two emerging and complementary techniques able to provide interaction kinetic information, in near physiological conditions and without any labelling. Both approaches show that p53R175H forms a very specific and highly stable bimolecular complex with both p63 and p53; with these interactions being characterized by a very high affinity with equilibrium dissociation constant, K_D, of about 10^{-9} M. These kinetics results, discussed also in connection with those previously reported for the interaction of p53R175H with p73, could inspire the design of suitable anticancer drugs able to antagonize the interaction of p53R175H with the p53 family members, by restoring then their anti-tumour function.

1. Introduction

p53, the "guardian of the genome", is a master regulator of cellular processes such as apoptosis, DNA repair and cell cycle [1]. Furthermore it is an important tumour suppressor which is found to be mutated or down-regulated in most cancer cells [2]. p53 down-regulation is driven by inhibitors through transcriptional inactivation and proteasomal degradation [3]. Some of the most important inhibitors are ubiquitin ligases such as MDM2 and COP1 [4], whose interaction with p53 has been regarded as a promising target for new anticancer strategies [5–8].

* Corresponding author at: Biophysics & Nanoscience Centre, DEB, Università della Tuscia, Largo dell'Università, 01100 Viterbo, Italy.
E-mail address: cannistr@unitus.it (S. Cannistraro).

http://dx.doi.org/10.1016/j.bpc.2017.07.002
Received 2 May 2017; Received in revised form 3 July 2017; Accepted 3 July 2017
Available online 05 July 2017
0301-4622/

Moreover, p53 is the most frequently mutated gene in cancer cells and its mutants are frequently associated with poor prognosis and drug resistance in several malignancies [9–11]. Since the mutations are mainly located in its DNA binding domain, mutant p53 proteins lose the ability to fully recognize the DNA consensus sequence for wild type p53 (p53wt); indeed, some mutants of p53 may gain new functions that promote tumorigenesis upon regulation of different target genes or by altering the interaction with p53wt partners [12–14]. However in case of p53 inactivation, other members of its family, namely p63 and p73 which share high structural homology with it, are able to vicariate the oncosuppressive function of p53 by regulating cell proliferation, differentiation and apoptosis [15,16]. Unfortunately, some mutants of p53 have been shown to inhibit the anti-tumour function of both p63 and p73 [17–21]. In particular, p53R175H, which is one of the most frequent p53 mutant found in many tumours such as colorectal and breast cancer [11], is able to interact with p73 *in vivo* with consequent abrogation of the protective function of the latter [17,18,20]. The *in vitro* kinetic characterization of the p53R175H/p73 complex has been found to be consistent with a high affinity interaction and has provided some insights for the design of specific drugs to prevent the interaction of these two partners [22]. In addition, p53R175H has been shown to inhibit the p63 transcriptional activity and, consequently, its tumour suppressive functions [19]. In this respect, the elucidation of the kinetics of their association might contribute to the design of novel anticancer drugs which could antagonize p53R175H and make p63 available for anti-tumour effects. Furthermore, it has been found that the oncogenic mutant p53R175H impairs the p53wt tumour suppressive function even when this is still present, although the mechanism underlying such a dominant negative effect is still highly debated [21,23–25]. Therefore, it could be very interesting to investigate the kinetic details of their interaction. Keeping in mind the crucial role of the mutant p53R175H in determining the inhibition of the oncosuppressive function of p53wt and of its sibling p63, and with the aim at providing some insight on the design of interaction antagonist drugs, we have performed a kinetic study of p53R175H/p53wt and of p53R175H/p63 complexes by using Surface Plasmon Resonance (SPR) and Atomic Force Spectroscopy (AFS), which are two innovative and complementary techniques operating *in vitro* in nearly native conditions. SPR is a powerful tool able to monitor molecular interactions in bulk without using labels and to characterize kinetic parameters and affinity of binding processes occurring between a sensor chip immobilized ligand and its partner free in solution [26]. On the other hand, AFS is a nanotechnology-based approach which studies interactions between one single couple of partners with a picoNewton sensitivity and allows to evaluate kinetics and energy landscape of the biocomplex formation [27]. Both techniques showed the occurrence of a specific interaction of p53R175H with both p53wt and p63. The equilibrium dissociation constant (K_D) of the two biomolecular complexes was measured to be about 10^{-9} M, such as a value being typical of high affinity interactions similarly to what found for the cognate p53R175H/p73 complex and the p53wt homodimeric complex [22,28].

2. Material and methods

2.1. Materials

Wild type human Glutathione S-Transferase (GST)-tagged p53 (80 kDa) (p53wt) and human GST-tagged p63 (90 kDa) (p63) were purchased from Sigma Aldrich (Saint Louis, Missouri, US). Human tag free p53R175H (43 kDa) was purchased from GenScript (Piscataway, NJ, US) by using the BacPower™ Guaranteed Bacterial Protein Expression Service.

2.2. SPR substrate preparation

SPR analysis were performed with a Biacore X100 instrument (GE Healthcare, Bio-Sciences AB, Sweden) at 25 °C. In different experiments, p53wt or p63 was immobilized onto a CM5 sensor chip surface (GE Healthcare, Little Chalfont, UK) by using the GST Capture Kit (GE Healthcare), following the procedure recommended by the producer and previously described [29]. This strategy involves a capturing molecule covalently immobilized on the surface in order to attach ligand by high affinity binding. To this aim the anti GST antibody (GE Healthcare) was immobilized by using a standard amine coupling chemistry [30]. Briefly, the carboxymethylated dextran surface of the CM5 sensor chip (GE Healthcare) was first activated by a 7 minute injection of a 1:1 mixture of 0.4 M *N*-ethyl-*N*-(3-diethylaminopropyl) carbodiimide (EDC) and 0.1 M *N*-hydroxyl-succinimide (NHS) at 10 μl/min to give reactive succinimide esters. Then a solution of anti GST antibody (30 μg/μl) in immobilization buffer (10 mM sodium acetate pH 5.0, GE Healthcare) was fluxed over the reactive matrix using a flow rate of 10 μl/min. In such a way, the NHS esters reacted spontaneously with the ligand amines to form covalent links (Fig. 1A). We immobilized about 7500 Resonance Units (RU) of anti-GST antibody in Flow cell 1 (Fc1) and 2 (Fc2). Unreacted sites were blocked by injecting for 7 min 1 M ethanolamine-HCl pH 8.5 (GE Healthcare) with a flow rate of 10 μl/min. Since the anti-GST antibody has high affinity sites which could negatively interfere with the analysis, these sites were inactivated as suggested by the producer; in particular, recombinant GST (5 μg/ml in 50 mM Phosphate Buffered Saline (PBS) pH 7.4, hereafter PBS buffer, GE Healthcare) was injected for 3 min, then regeneration solution (10 mM glycine-HCl pH 2.1, GE Healthcare) was flowed for 2 min and this procedure was repeated twice. The two flow cells were immobilized by using identical conditions; therefore Fc2 was used for ligand capture while the Fc1 was used as reference. In the Fc2, after the baseline was stabilized by fluxing the running buffer (PBS buffer, 0.005% surfactant P20, GE Healthcare) over the surface, the ligand, p53wt (0.1 μM in running buffer) or p63 (0.2 μM in running buffer), was injected at 10 μl/min flow rate until reaching an immobilized ligand level (R) of about 150 and 160 RU for p53wt and p63, respectively, with a theoretical analyte binding capacity (R_{max}) of about 80 RU for both.

R_{max} was calculated by using the following equation:

$$R_{max} = \left(\frac{Analyte\ MW}{Ligand\ MW}\right)R \quad (1)$$

where analyte MW is the molecular weight of p53R175H and ligand MW is the molecular weight of p53wt or p63. To prevent non-specific binding of the analyte, p53R175H, with the anti GST antibody, we injected recombinant GST (20 μg/ml), blocking the anti-GST antibody sites which did not react with the ligand in the Fc2 and saturating all the anti GST binding sites in the Fc1. A schematic representation of the immobilization procedures of Fc1 and Fc2 is shown in Fig. 1B and C, respectively.

2.3. SPR binding experiment

SPR analyses were performed by using a single-cycle kinetics approach which consists in sequential injections of increasing concentrations of the analyte over the functionalized sensor chip surface, without regeneration steps between each sample injection [31]. By using a flow rate of 30 μl/min, five sequential increasing concentrations (33.3, 66.6, 100, 200 and 400 nM) of p53R175H solution were fluxed over the sensor chip surface for 160 s, followed by a 160 s dissociation with running buffer and a final dissociation of 400 s with the same buffer, without intermediate regeneration. Finally, the substrate was regenerated by using a 2 minute pulse of regeneration solution at 10 μl/min. Analytical cycles were programmed by means of a wizard template and the entire analysis was completely automated. A sketch of the p53R175H interaction over the p63 or the p53wt functionalized substrate is shown in Fig. 1D. The BiaEvaluation software 2.1 (GE

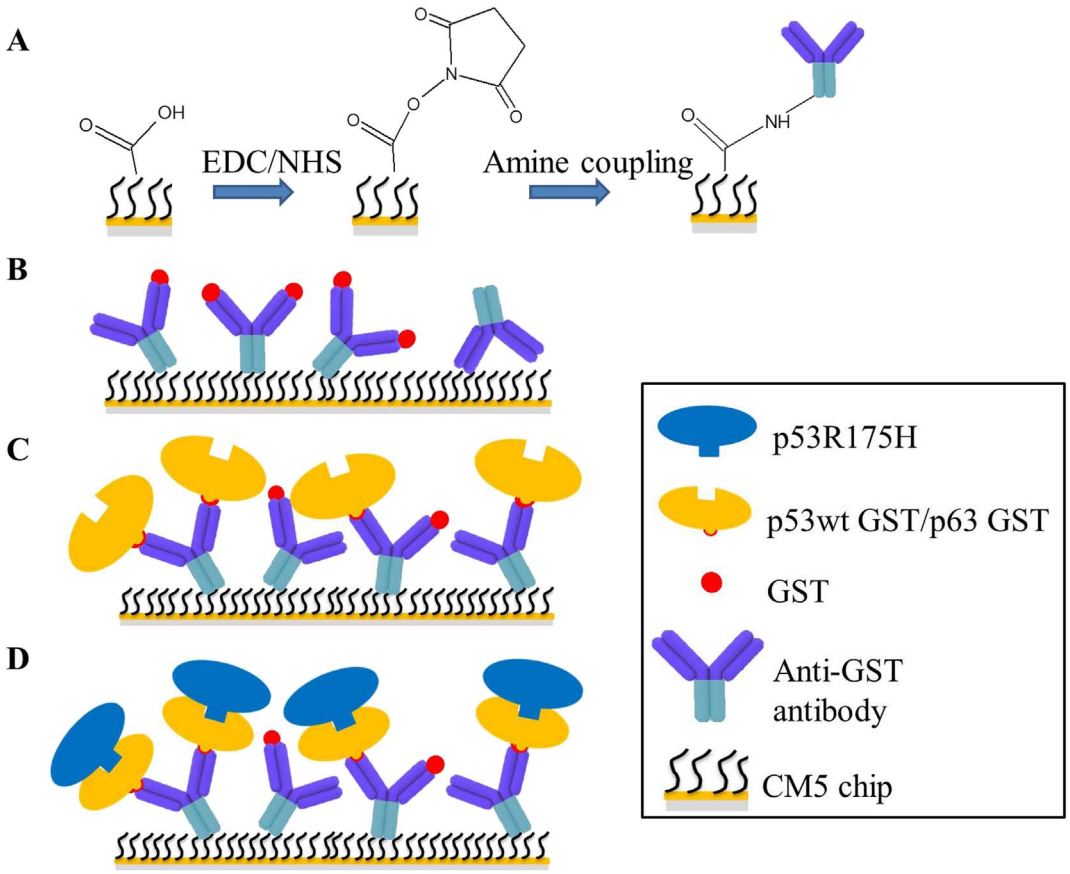

Fig. 1. SPR experiment: immobilization procedure and binding assay. A, the CM5 dextran matrix was activated by injecting a mixture of *N*-ethyl-*N*-(3-diethylaminopropyl) carbodiimide (EDC) and *N*-hydroxyl-succinimide (NHS), then the amine coupling was obtained. The amino groups of anti GST antibody, which was fluxed over the active surface, spontaneously reacted with the *N*-hydrosuccinimide esters of the substrate to form covalent links. B, anti GST antibody sites were saturated with GST in the reference Flow cell 1. C, the p63-GST or the p53wt-GST was captured by anti GST antibody, then the antigen sites were saturated with GST in the Flow cell 2 (Fc2). D, during binding experiments p53R175H interacted with p63 or p53wt in the Fc2.

Healthcare) was used to extract kinetic parameters from SPR data. The reference surface, Fc1, was used to correct for systematic noise and instrument drift. The binding assay also included three start up cycles using buffer to equilibrate the surface, as well as a zero concentration cycle of analyte in order to have a blank response usable for double reference subtraction [32]. The SPR response as a function of time (sensorgram) was then globally fitted to a 1:1 interaction model including the correction for mass transfer rate [33]. The goodness of the fit was evaluated by χ^2 value and residual plots.

2.4. AFS experimental procedure and analysis

Silicon nitride AFM tips (MSNL-10, Bruker, Billerica, MA, USA) and 2D–Aldehyde functionalized glass surfaces (PolyAn GmbH, Berlin, Germany) were used to covalently link p53R175H and p53wt or p63, respectively (Fig. 2A). In particular, we used 10 μl of a 5 μM solution of p53R175H for tip functionalization according to the procedure previously reported [34]. Briefly, tips were cleaned in acetone for 10 min, dried with nitrogen and then UV irradiated for 30 min. Then, they were

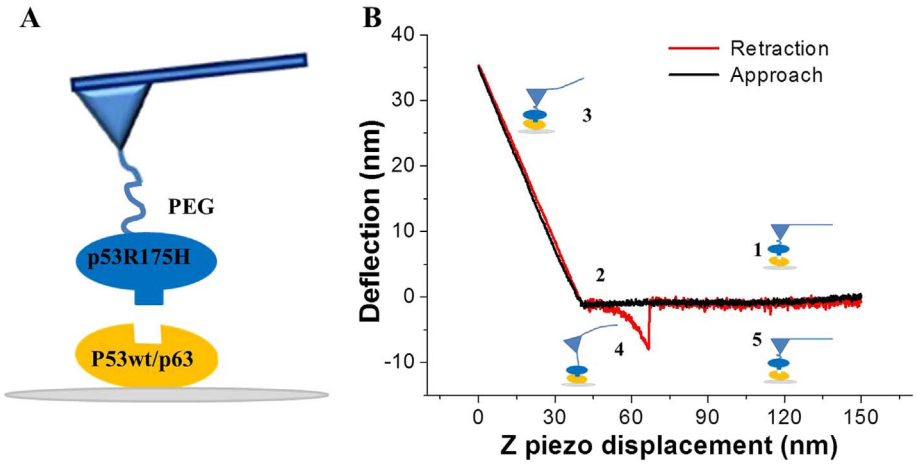

Fig. 2. Schematic representation of AFS experiment. A, Sketch of the p53R175H linked to the cantilever by using a polyethylene glycol (PEG) linker and of the p53wt or p63 immobilized onto the functionalized glass substrate. B, A typical approach-retraction cycle, showing a specific unbinding event.

immersed in a solution of 2% (v/v) 3-mercatopropyl-trimethoxysilane (Sigma Aldrich) in toluene for 2 h at room temperature and extensively washed with toluene. Subsequently, the silanized tips were incubated with a solution of 1 mM *N*-hydroxysuccinimide-polyethylenglycol-maleimide (NHS-PEG-MAL, MW 3400 Da, N = 24) (Thermo Fisher Scientific, Waltham, Massachusetts, USA) in DMSO for 3 h at room temperature and were rinsed in DMSO to remove the unbound PEG. This spacer contains a thiol-reactive group (MAL) at one end, to link silane molecules, and an amino-reactive group (NHS) at the other end, to couple $-NH_2$ groups of lysines exposed on the protein surface. Therefore, tips were incubated with 10 μl of p53R175H (5 μM) in PBS buffer overnight at 4 °C, then they were gently rinsed with PBS buffer and subsequently with Milli-Q water.

Furthermore, 2D-Aldehyde functionalized glass surfaces, characterized by a thin silane layer able to covalently bind most types of biomolecules, were used for substrate preparation by incubating a 1 cm^2 glass slide with 20 μl of p53wt or p63 (5 μM) in PBS buffer overnight at 4 °C. Then, the substrate was rinsed with PBS buffer and Milli-Q water. Finally, to passivate unreacted groups, both tips and substrates were incubated with 1 M ethanolamine-HCl, pH 8.5 (GE Healthcare) in Milli-Q water for 30 min at room temperature, gently rinsed with PBS buffer and Milli-Q water and then used for the AFS experiment or stored in PBS buffer at 4 °C.

Force measurements were performed at room temperature with a commercial AFM (Nanoscope IIIa/Multimode AFM, Veeco Instruments, Plainview, NY, USA) in PBS buffer in a force calibration mode. Force curves were acquired by using rectangular-shaped cantilevers (MSNL-10 cantilever B) with a nominal spring constant, k_{nom}, of 0.02 N/m. A ramp size of 150 nm was set up and an encounter time of 100 ms was established. A relative trigger of 35 nm was used to limit at 0.7 nN the maximum contact force applied by the tip on the protein functionalized substrate. Fig. 2B shows an approach- retraction cycle: at the beginning the p53R175H-functionalized tip was moved toward the p53wt/p63-functionalized substrate (point 1). The biomolecules jumped-to-contact at point 2. With further pressure of the tip onto the substrate, there was an electronic repulsion due to overlapping of molecular orbitals, producing an upward deflection of the cantilever. Once the preset maximum contact force value was reached, the approaching phase (black curve) of the cantilever was stopped (point 3). Then, the cantilever was retracted from the substrate. During this retraction phase (red curve), adhesion forces and/or bonds formed in the contact phase caused the tip to bend downward, adhering to the substrate up to some distance beyond the initial contact point (point 4). As retraction continues, the spring force overcame the interacting force and the cantilever jumped off, sharply returning to a non-contact position (point 5). Force curves were collected by approaching the functionalized tip to different points of the substrate at a constant velocity of 50 nm/s, while the retraction velocity was varied from 50 to 4200 nm/s, according to the selected nominal loading rates, defined as the product of the nominal cantilever spring constant (k_{nom}) by the tip pulling velocity (ν), and set in the range of 1 to 84 nN/s. The effective loading rates were then calculated from the product between the pulling velocity, ν, by the spring constant of the entire system, k_{syst}, that was determined from the slope of the retraction trace of the force curves immediately prior to the jump-off of an unbinding event, thus allowing us to take into account the effect of the molecules (*i.e.*, proteins and/or linkers) tied to the tip [35]. To obtain a reliable quantitative information with statistical significance from the experiments, thousands of force curves were acquired at each loading rate. The exerted force, which was able to break the complex, called the unbinding force, *F*, could be calculated by multiplying the cantilever deflection at the jump-off by its effective spring constant (k_{eff}), which was, in turn, determined by the non-destructive thermal noise method [36]. The force curves registered during the measurements showed different shapes. Curves corresponding to acceptable unbinding events were characterized, in the retraction phase, by sharp peaks, starting and ending points at zero deflection line, and by a nonlinear curved shape before the jump-off, which was related to the stretching features of the PEG linker [37] as shown in Fig. 2B. Additionally, somewhat ambiguous deflection jumps were determined by using the 1/f noise approach [38,39].

3. Results

3.1. Kinetic results of p53R175H/p63 interaction by SPR

The interaction kinetics between p53R175H and p63 was studied in bulk by following a single-cycle kinetics SPR approach [31]. In particular, the analyte, p53R175H, was injected at five progressively higher concentrations (from 33.3 nM to 400 nM) over the ligand, p63, which had been previously immobilized by immunocapture as described in the Materials and Methods section, without any regeneration step. The SPR response (RU) as a function of time, namely the sensorgram, is shown in Fig. 3 (black dotted curve). The rise of the response signal after the first analyte injection indicated the formation of a complex between p53R175H and p63. Upon buffer injection, the signal slightly decreased and then reached a stable value, which is indicative of the persistence of a tight p53R175H/p63 complex. The same trend was observed for the successive injections: as far as higher p53R175H concentrations were used, progressively higher response values at the stability were obtained; with this being indicative of increasing levels of p53R175H bound to p63. To extract information on the kinetics of the p53R175H/p63 interaction, the sensorgram was analysed in the framework of the Langmuir 1:1 binding model, which assumes a simple reversible bimolecular reaction between the ligand and the analyte [40,41]. The model was modified to take into account for the mass transport effect [33]. In particular, it was assumed that the analyte is transferred from the bulk solution (A_{bulk}) toward the sensor chip surface, and *vice versa*, with a mass transfer coefficient (k_t), which is the same in both directions. Then, the analyte that has reached the sensor chip surface ($A_{surface}$), binds to the ligand, resulting in the formation of the ligand–analyte complex (*LA*) characterized by the association (k_{on}) and dissociation (k_{off}) rate constants according to:

$$A_{bulk} \underset{k_t}{\overset{k_t}{\rightleftarrows}} A_{surface} + L \underset{k_{off}}{\overset{k_{on}}{\rightleftarrows}} LA \qquad \text{(Scheme 1)}$$

The variation of $A_{surface}$, *L* and *LA* concentrations with time can be

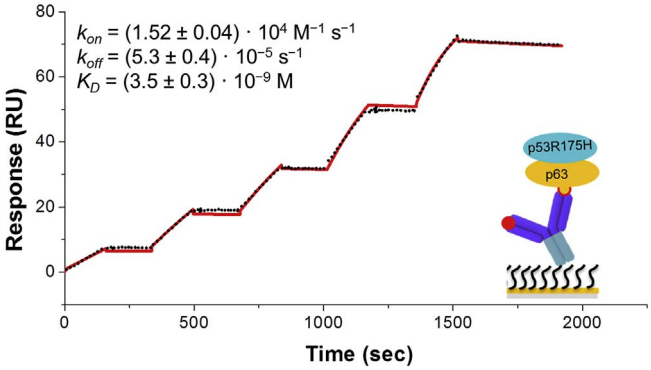

Fig. 3. SPR kinetic characterization of the interaction between p53R175H and p63. The sensorgram (black dotted curve) of the single-cycle kinetics assay shows the response (Resonance Unit, RU) growth after injecting five increasing concentrations (33.3, 66.6, 100, 200, 400 nM) of p53R175H over the p63 functionalized substrate, without any regeneration step. The red solid curve overlaid on the experimental data was obtained by fitting the sensorgram with the 1:1 binding model (BiaEvaluation software). The upside left inset shows the association rate constant (k_{on}), the dissociation rate constant (k_{off}) and the equilibrium dissociation constant (K_D) resulting from the fitting procedure. A schematic representation of the binding experiment is also shown (bottom, right). (For interpretation of the references to colour in this figure legend, the reader is referred to the web version of this article.)

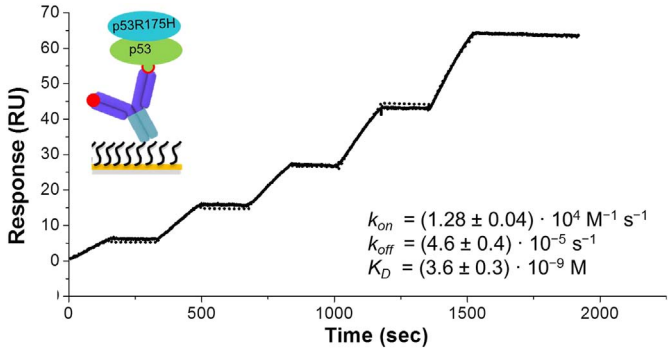

Fig. 4. SPR kinetic characterization of the interaction between p53R175H and p53wt. The sensorgram (black dotted curve) shows the response (Resonance Units, RU) *versus* time of the single-cycle kinetics assay performed by injecting five increasing concentrations (33.3, 66.6, 100, 200, 400 nM) of p53R175H over the p53wt substrate, without any regeneration. The black solid curve was obtained by fitting data with the 1:1 binding model (BiaEvaluation software). The bottom right inset shows the association rate constant (k_{on}), the dissociation rate constant (k_{off}), and the equilibrium dissociation constant (K_D) obtained from the fitting procedure. A schematic representation of the binding experiment is also shown (upside, left).

described by the following set of differential equations:

$$\frac{d[A_{Surface}]}{dt} = k_t([A_{bulk}] - [A_{surface}]) - (k_{on}[L][A_{surface}] - k_{off}[LA])$$
$$\frac{d[L]}{dt} = -(k_{on}[L][A_{surface}] - k_{off}[LA])$$
$$\frac{d[LA]}{dt} = (k_{on}[L][A_{surface}] - k_{off}[LA]) \quad (2)$$

To extract the kinetic parameters k_{on} and k_{off} the sensorgram was fitted according to a non-linear least square analysis and numerical integration of Eq. (2) [32] by using the BiaEvaluation software package. The fitting curve (red solid curve) was overlaid on the sensorgram as shown in Fig. 3. A k_{on} value of $(1.52 \pm 0.04) \cdot 10^4\ M^{-1}\ s^{-1}$ and a k_{off} of $(5.3 \pm 0.4) \cdot 10^{-5}\ s^{-1}$ were obtained (analyte binding capacity, $R_{max} = 84$; $\chi^2 = 0.52$). Moreover, the lifetime, τ, of the p63/p53R175H complex, calculated as $\tau = 1 / k_{off}$, was of about 5 h. Finally, by using the equation $K_D = k_{off} / k_{on}$, an equilibrium dissociation constant, K_D, of $(3.5 \pm 0.3) \cdot 10^{-9}$ M was calculated.

3.2. Kinetic results of p53R175H/p53wt interaction by SPR

The kinetics of the interaction between the mutant p53R175H and p53wt was investigated in bulk by using the same approach followed for the p53R175H/p63 complex. Fig. 4 shows the sensorgram (black dotted curve) which resulted from the injection of 5 successive increasing concentrations (from 33.3 nM to 400 nM) of the analyte, p53R175H, over a sensor chip surface which had been previously functionalized with the ligand, p53wt. In particular, during each injection of p53R175H the response signal increased, indicating the formation of the p53R175H/p53wt complex; after the subsequent injection of buffer, a slow dissociation occurred and the response signal reached a stable value, revealing that a strong interaction between p53R175H and p53wt persisted. Moreover, after injecting higher concentrations of p53R175H, the sensorgram showed an increment of the response values at the stability, highlighting the increased amount of p53R175H bound to p53wt (Fig. 4), similarly to what previously shown for the p53R175H/p63 interaction (Fig. 3). Again, we fitted our data with a 1:1 binding model by using the BiaEvaluation software and the curve obtained from the fitting procedure (black solid curve) is shown overlaid on the experimental data in Fig. 4. Therefore, we found a k_{on} of $(1.28 \pm 0.04) \cdot 10^4\ M^{-1}\ s^{-1}$ and a k_{off} of $(4.6 \pm 0.4) \cdot 10^{-5}\ s^{-1}$, with a corresponding lifetime of about 6 h, and finally a K_D of $(3.6 \pm 0.3) \cdot 10^{-9}$ M ($R_{max} = 81$; $\chi^2 = 0.52$) was calculated.

3.3. Kinetics and energy landscape results of the interaction between p53R175H and p53wt or p63 by AFS

The interactions between the oncogenic mutant p53R175H and the two p53 family members, p53wt and p63, were investigated also by AFS at single molecule level by using a p53R175H functionalized tip and a p53wt or p63 conjugated substrate prepared as described in the Material and Methods section. The analysis of AFS curves, collected at five increasing loading rates, was performed as previously described [42]. In particular, the unbinding forces of the selected curves were evaluated and cast into a histogram for each loading rate; in all the cases a single mode distribution was obtained and the most probable unbinding force (F^*) was extracted from the maximum of the peak of the corresponding histogram. Fig. 5A shows a representative histogram corresponding to 1.5 nN/s loading rate, similar histograms were obtained at the other loading rates. The recorded F^* increased with the loading rate with values varying between 40 and 50 pN, which were in the range usually reported for specific biological interactions [43]. The unbinding frequency, calculated as the ratio between the number of events corresponding to specific unbinding processes over the total recorded events, was about 10%, being consistent with values previously reported for other protein-protein interactions [29,44]. The unbinding process to which the p53R175H/p53wt complex undergoes induced by the external loading force can be treated within the theoretical context of the Bell- Evans model [45,46]. Accordingly, the application of an external force (F^*) modifies the energy profile of the unbinding process, lowering the activation energy barrier. The model comply with a linear dependence of the F^* on the natural logarithm of the loading rate, r, as given by the following equation:

$$F^* = \frac{k_B T}{x_\beta} \ln\left(\frac{r\, x_\beta}{k_{off} k_B T}\right) \quad (3)$$

where k_B is Boltzmann's constant, T is the absolute temperature, k_{off} is the dissociation rate constant and x_β is the width of the energy barrier along the direction of the applied force. By plotting F^* *versus* the logarithm of the effective loading rate r, we observed a single regime

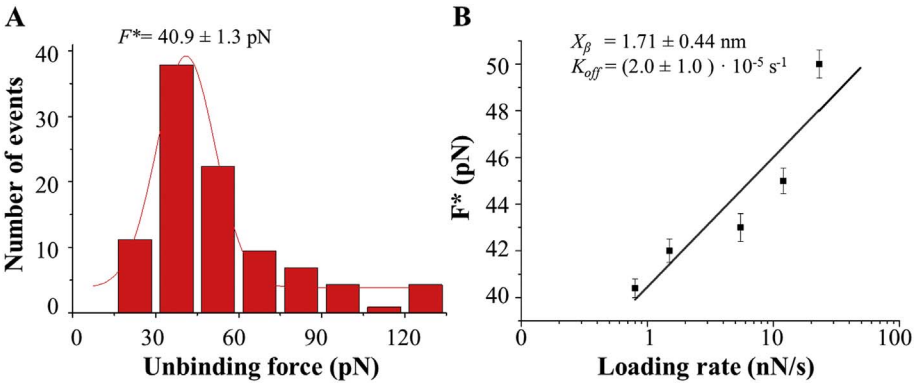

Fig. 5. Analysis of AFS results for the p53R175H/p53wt complex. A, Histograms of the unbinding force at a loading rate of 1.5 nN/s. The most probable unbinding force value (F^*) was determined from the maximum of the main peak of the histogram of unbinding forces by fitting with Gaussian function (black curve). B, Plot of the most probable unbinding forces, F^*, *versus* the logarithm of the loading rates for the p53R175H/p53wt interaction. The line is obtained by fitting the experimental data by the Bell–Evans model. The resulting dissociation rate constant, k_{off}, and the width of the energy barrier along the direction of the applied force, x_β, are shown in the insert.

indicative of a single energy barrier and unique transition state of the reaction (Fig. 5B). Moreover, by fitting these data with Eq. (3), we found a x_β of (1.71 ± 0.44) nm and a k_{off} of $(2.0 \pm 1.0) \cdot 10^{-5}\,s^{-1}$ (Fig. 5B). Interestingly, we found a lifetime of about 14 h for the p53R175H/p53wt interaction. To complete the kinetic profile of the interaction, we also estimated the association rate constant (k_{on}) of the p53R175H/p53wt complex according to the expression $k_{on} = N_A \cdot V_{eff} / t_{0.5}$, where N_A is the Avogadro's number, V_{eff} is the effective volume of a half-sphere with radius r_{eff} around the tip, and $t_{0.5}$ is the time for the half-maximal binding probability, given by $t_{0.5} = 2\, r_{eff} / v$, where v is the approach speed of the cantilever, as detailed in [47,48]. Accordingly, a k_{on} of about $10^4\,M^{-1}\,s^{-1}$ was obtained. The assessment of both the dissociation and association rate constants allowed to calculate a K_D of about 10^{-9} M for the p53R175H/p53wt complex.

We used the same AFS approach also for the analysis of the p53R175H/p63 interaction (data not shown). We found a single energy barrier and a unique transition state of the reaction characterized by a x_β of (1.68 ± 0.42) nm and a k_{off} of $(3.0 \pm 1.0) \cdot 10^{-5}\,s^{-1}$. Moreover, we found a lifetime of about 9 h and, by applying the same procedure described above for the p53R175H/p53wt complex, we calculated a k_{on} of about $10^4\,M^{-1}\,s^{-1}$ and finally a K_D of about 10^{-9} M.

4. Discussion

In the present study, we highlighted the occurrence of a strong bimolecular complex between p53R175H and p63 both in bulk and at single molecule by using SPR and AFS, respectively. The corresponding kinetic parameters, which were indeed missing in the literature, witnessed a very high affinity interaction, characterized by a K_D in the 10^{-9} M concentration range; with such a value being comparable with that of antigen-antibody pairs [49,50]. The p53R175H/p63 complex showed a k_{off} value of $10^{-5}\,s^{-1}$ and a wide energy barrier, typical of specific and strong biological complexes [27]. Furthermore, this complex showed a long lifetime of several hours, confirmed by both techniques, which might be crucial for the impairment of the p63 function. A somewhat similar kinetics and high affinity, was observed for the interaction between p53R175H and the other member of p53 family, p73, by using the same techniques [22]. Indeed, the higher affinity found for the p53R175H/p63 complex by SPR, with respect to that of the p53R175H/p73 complex, could be traced back to the presence of a specific aggregating peptide identified in the p63 sequence [23], which might be responsible for a stronger interaction with p53R175H. We also demonstrated the occurrence of a bimolecular complex between the oncogenic mutant p53R175H and p53wt, whose kinetic parameters were also unknown. Notably, the strong stability ($k_{off} = 10^{-5}\,s^{-1}$) and high affinity ($K_D = 10^{-9}$ M) of this complex, confirmed by both AFS and SPR results, are very similar to those of the p53R175H/p63 complex and could be significantly relevant to the oncogenic function of the p53 mutant. It would be interesting to discuss this result in connection with the p53wt/p53wt homodimer interaction which was shown to play a pivotal role in the oncosuppressive function of p53 *in vivo* [51]. In this context, we wonder if the observed p53R175H/p53wt interaction could antagonize the homodimer formation. Actually, the two complexes share a comparable high affinity ($K_D = 10^{-9}$ M), but the dissociation rate of the homodimer is much faster than that of the p53R175H/p53wt complex [28]. Therefore, the formation of the p53R175H/p53wt complex could be prevalent, especially when high levels of p53R175H accumulates in cancer cells, leading to the impairment of the functional p53wt homodimer. The strong interaction of the mutant p53R175H with all the p53 family members could trigger the sequestering of the p53 family members, leading to the dominant negative effect shown by this mutant [21,23–25]. Our results could also indicate that the molecular mechanism underlying the formation of p53R175H/p53wt and p53R175H/p63 complexes is quite similar as proposed by Xu et al. [21]. Indeed, these authors suggested that it is the same exposed peptide belonging to the mutant p53R175H which is involved in the interaction with the DNA binding domain of all the p53 family members. Kehrloesser et al. [23] showed instead that different domains could be involved in the formation of p53R175H/p63 and p53R175H/p53wt complexes; the former being mediated by the C-terminal transactivation inhibitory domain of p63; while the latter, being based on the involvement in the interaction of the p53 oligomerization domain.

5. Conclusions

Collectively, our results highlight the peculiar ability of the oncogenic mutant p53R175H to form high affinity complexes with both p63 and p53wt. Remarkably, these results may provide some insights on anticancer strategies aimed at targeting the bimolecular interaction between the oncogenic mutant p53R175H and the p53 family members. In particular, small molecules or peptides, suitably designed to bind to this mutant with an affinity comparable or higher than that shown by this mutant for p53wt and p63, could be rewarding anticancer drugs able to restore the oncosuppressive activity of p53 and of its vicars, p63 and p73.

Acknowledgments

This work was supported by the Italian Association for Cancer Research (AIRC) (Grant IG15866 to SC).

References

[1] D.P. Lane, Cancer. p53, guardian of the genome, Nature 358 (1992) 15–16.
[2] B. Vogelstein, D. Lane, A.J. Levine, Surfing the p53 network, Nature 408 (2000) 307–310.
[3] J.P. Kruse, W. Gu, Modes of p53 regulation, Cell 137 (2009) 609–622.
[4] C.L. Brooks, W. Gu, p53 regulation by ubiquitin, FEBS Lett. 585 (2011) 2803–2809.
[5] F. Domenici, M. Frasconi, F. Mazzei, G. D'Orazi, A.R. Bizzarri, S. Cannistraro, Azurin modulates the association of Mdm2 with p53: SPR evidence from interaction of the full-length proteins, J. Mol. Recognit. 24 (2011) 707–714.
[6] L.T. Vassilev, Small-molecule antagonists of p53-MDM2 binding: research tools and potential therapeutics, Cell Cycle 3 (2004) 419–421.
[7] M. Wade, Y.C. Li, G.M. Wahl, MDM2, MDMX and p53 in oncogenesis and cancer therapy, Nat. Rev. Cancer 13 (2013) 83–96.
[8] T. Yamada, K. Christov, A. Shilkaitis, L. Bratescu, A. Green, S. Santini, A.R. Bizzarri, S. Cannistraro, T.K.D. Gupta, C.W. Beattie, p28, a first in class peptide inhibitor of cop1 binding to p53, Br. J. Cancer 108 (2013) 2495–2504.
[9] C. Kandoth, M.D. McLellan, F. Vandin, K. Ye, B. Niu, C. Lu, M. Xie, Q. Zhang, J.F. McMichael, M.A. Wyczalkowski, M.D.M. Leiserson, C.A. Miller, J.S. Welch, M.J. Walter, M.C. Wendl, T.J. Ley, R.K. Wilson, B.J. Raphael, L. Ding, Mutational landscape and significance across 12 major cancer types, Nature 502 (2013) 333–339.
[10] R. Brosh, V. Rotter, When mutants gain new powers: news from the mutant p53 field, Nat. Rev. Cancer 9 (2009) 701–713.
[11] A. Petitjean, E. Mathe, S. Kato, C. Ishioka, S.V. Tavtigian, P. Hainaut, M. Olivier, Impact of mutant p53 functional properties on TP53 mutation patterns and tumor phenotype: lessons from recent developments in the IARC TP53 database, Hum. Mutat. 28 (2007) 622–629.
[12] W.A. Freed-Pastor, C. Prives, Mutant p53: one name, many proteins, Genes Dev. 26 (2012) 1268–1286.
[13] M. Ferraiuolo, S. Di Agostino, G. Blandino, S. Strano, Oncogenic intra-p53 family member interactions in human cancers, Front. Oncol. 6 (2016) 77.
[14] D. Walerych, K. Lisek, G. Del Sal, Mutant p53: one, no one, and one hundred thousand, Front. Oncol. 5 (2015) 289.
[15] L. Collavin, A. Lunardi, G. Del Sal, p53-family proteins and their regulators: hubs and spokes in tumor suppression, Cell Death Differ. 17 (2010) 901–911.
[16] M.P. Deyoung, L.W. Ellisen, p63 and p73 in human cancer: defining the network, Oncogene 26 (2007) 5169–5183.
[17] C.J. Di Como, C. Gaiddon, C. Prives, p73 function is inhibited by tumor-derived p53 mutants in mammalian cells, Mol. Cell. Biol. 19 (1999) 1438–1449.
[18] C. Gaiddon, M. Lokshin, J. Ahn, T. Zhang, C. Prives, A subset of tumor-derived mutant forms of p53 down-regulate p63 and p73 through a direct interaction with the p53 core domain, Mol. Cell. Biol. 21 (2001) 1874–1887.
[19] S. Strano, G. Fontemaggi, A. Costanzo, M.G. Rizzo, O. Monti, A. Baccarini, G. Del Sal, M. Levrero, A. Sacchi, M. Oren, G. Blandino, Physical interaction with human tumor-derived p53 mutants inhibits p63 activities, J. Biol. Chem. 277 (2002) 18817–18826.
[20] S. Strano, E. Munarriz, M. Rossi, B. Cristofanelli, Y. Shaul, L. Castagnoli, A.J. Levine, A. Sacchi, G. Cesareni, M. Oren, G. Blandino, Physical and functional interaction between p53 mutants and different isoforms of p73, J. Biol. Chem. 275 (2000)

29503–29512.
[21] J. Xu, J. Reumers, J.R. Couceiro, F. De Smet, R. Gallardo, S. Rudyak, A. Cornelis, J. Rozenski, A. Zwolinska, J.C. Marine, D. Lambrechts, Y.A. Suh, F. Rousseau, J. Schymkowitz, Gain of function of mutant p53 by coaggregation with multiple tumor suppressors, Nat. Chem. Biol. 7 (2011) 285–295.
[22] S. Santini, S. Di Agostino, E. Coppari, A.R. Bizzarri, G. Blandino, S. Cannistraro, Interaction of mutant p53 with p73: a Surface Plasmon Resonance and Atomic Force Spectroscopy study, Biochim. Biophys. Acta 1840 (2014) 1958–1964.
[23] S. Kehrloesser, C. Osterburg, M. Tuppi, B. Schäfer, K.H. Vousden, V. Dötsch, Intrinsic aggregation propensity of the p63 and p73 TI domains correlates with p53R175H interaction and suggests further significance of aggregation events in the p53 family, Cell Death Differ. 23 (2016) 1952–1960.
[24] G. Wang, A.R. Fersht, Propagation of aggregated p53: cross-reaction and coaggregation vs. seeding, Proc. Natl. Acad. Sci. U. S. A. 112 (2015) 2443–2448.
[25] O. Billant, A. Léon, S. Le Guellec, G. Friocourt, M. Blondel, C. Voisset, The dominant-negative interplay between p53, p63 and p73: a family affair, Oncotarget 7 (2016) 69549–69564.
[26] J. Homola, Surface plasmon resonance sensors for detection of chemical and biological species, Chem. Rev. 108 (2008) 462–493.
[27] A.R. Bizzarri, S. Cannistraro, Dynamic Force Spectroscopy and Biomolecular Recognition, CRC Press, Boca Raton, 2012.
[28] S. Rajagopalan, F. Huang, A.R. Fersht, Single-molecule characterization of oligomerization kinetics and equilibria of the tumor suppressor p53, Nucleic Acids Res. 39 (2011) 2294–2303.
[29] I. Moscetti, E. Teveroni, F. Moretti, A.R. Bizzarri, S. Cannistraro, MDM2-MDM4 molecular interaction investigated by atomic force spectroscopy and surface plasmon resonance, Int. J. Nanomedicine 11 (2016) 4221–4229.
[30] B. Johnsson, S. Löfås, G. Lindquist, Immobilization of proteins to a carboxymethyldextran-modified gold surface for biospecific interaction analysis in surface plasmon resonance sensors, Anal. Biochem. 198 (1991) 268–277.
[31] R. Karlsson, P.S. Katsamba, H. Nordin, E. Pol, D.G. Myszka, Analyzing a kinetic titration series using affinity biosensors, Anal. Biochem. 349 (2006) 136–147.
[32] T.A. Morton, D.G. Myszkaand, I.M. Chaiken, Interpreting complex binding kinetics from optical biosensors: a comparison of analysis by linearization, the integrated rate equation, and numerical integration, Anal. Biochem. 227 (1995) 176–185.
[33] R.W. Glaser, Antigen-antibody binding and mass transport by convection and diffusion to a surface: a two-dimensional computer model of binding and dissociation kinetics, Anal. Biochem. 213 (1993) 152–161.
[34] G. Funari, F. Domenici, L. Nardinocchi, R. Puca, G. D'Orazi, A.R. Bizzarri, S. Cannistraro, Interaction of p53 with Mdm2 and azurin as studied by atomic force spectroscopy, J. Mol. Recognit. 23 (2010) 343–351.
[35] C. Friedsam, A.K. Wehle, F. Kühner, H.E. Gaub, Dynamic single-molecule force spectroscopy: bond rupture analysis with variable spacer length, J. Phys. Condens. Matter 15 (2003) S1709.
[36] J.L. Hutter, J. Bechhoefer, Calibration of atomic-force microscope tips, Rev. Sci. Instrum. 64 (1993) 1868–1873.
[37] F. Kienberger, A. Ebner, H.J. Gruber, P. Hinterdorfer, Molecular recognition imaging and force spectroscopy of single biomolecules, Acc. Chem. Res. 39 (2006) 29–36.
[38] A.R. Bizzarri, S. Cannistraro, Antigen–antibody biorecognition events as discriminated by noise analysis of force spectroscopy curves, Nanotechnology 25 (2014) 335102.
[39] A.R. Bizzarri, S. Cannistraro, $1/f^{\alpha}$ noise in the dynamic force spectroscopy curves signals the occurrence of biorecognition, Phys. Rev. Lett. 110 (2013) 048104.
[40] P. Björquist, S. Boström, Determination of the kinetic constants of tissue factor/factor VII/factor VIIA and antithrombin/heparin using surface plasmon resonance, Thromb. Res. 85 (1997) 225–236.
[41] D.J. O'Shannessy, M. Brigham-Burke, K.K. Soneson, P. Hensley, I. Brooks, Determination of rate and equilibrium binding constants for macromolecular interactions using surface plasmon resonance: use of nonlinear least squares analysis methods, Anal. Biochem. 212 (1993) 457–468.
[42] A.R. Bizzarri, S. Cannistraro, The application of atomic force spectroscopy to the study of biological complexes undergoing a biorecognition process, Chem. Soc. Rev. 39 (2010) 734–749.
[43] J. Morfill, K. Blank, C. Zahnd, B. Luginbühl, F. Kühner, K.E. Gottschalk, A. Plückthun, H.E. Gaub, Affinity-matured recombinant antibody fragments analyzed by single-molecule force spectroscopy, Biophys. J. 93 (2007) 3583–3590.
[44] E. Coppari, S. Santini, A.R. Bizzarri, S. Cannistraro, Kinetics and binding geometries of the complex between β2-microglobulin and its antibody: an AFM and SPR study, Biophys. Chem. 211 (2016) 19–27.
[45] G.I. Bell, Models for the specific adhesion of cells to cells, Science 200 (1978) 618–627.
[46] E. Evans, K. Ritchie, Dynamic strength of molecular adhesion bonds, Biophys. J. 72 (1997) 1541–1555.
[47] A.R. Bizzarri, S. Santini, E. Coppari, M. Bucciantini, S. Di Agostino, T. Yamada, C.W. Beattie, S. Cannistraro, Interaction of an anticancer peptide fragment of azurin with p53 and its isolated domains studied by atomic force spectroscopy, Int. J. Nanomedicine 6 (2011) 3011–3019.
[48] M. Taranta, A.R. Bizzarri, S. Cannistraro, Probing the interaction between p53 and the bacterial protein azurin by single molecule force spectroscopy, J. Mol. Recognit. 21 (2008) 63–70.
[49] J.P. Landry, Y. Ke, G.L. Yu, X.D. Zhu, Measuring affinity constants of 1450 monoclonal antibodies to peptide targets with a microarray-based label-free assay platform, J. Immunol. Methods 417 (2015) 86–96.
[50] I.M.A. Nooren, J.M. Thornton, Diversity of protein-protein interactions, EMBO J. 22 (2003) 3486–3492.
[51] G. Gaglia, Y. Guan, J.V. Shah, G. Lahav, Activation and control of p53 tetramerization in individual living cells, Proc. Natl. Acad. Sci. U. S. A. 110 (2013) 15497–15501.